A New 1,3,4-Oxadiazole-based Hole Transport Material for Efficient $CH_3NH_3PbBr_3$ Perovskite Solar Cells: Facile Synthesis and Energy Level Alignment

Stefano Carli,*[a] Juan Pablo Correa Baena,*[b] Giulia Marianetti,[c] Antonio Abate,[d] Stefano Caramori,[a] Michael Grätzel,[d] Fabio Bellina,[e] Carlo Alberto Bignozzi,[a] Anders Hagfeldt[b]

Abstract: *A new hole transport material based on the 1,3,4-oxadiazole moiety (H1) has been prepared through a one-step synthetic pathway starting from commercially available products. Thanks to its deep HOMO level, H1 was used as hole transport material (HTM) on $CH_3NH_3PbBr_3$ ($MAPbBr_3$) perovskite solar cells yielding a J-V hysteresis-free efficiency of 5.8%, while the reference material (Spiro-OMeTAD), in the same testing conditions, furnished a lower efficiency of 5.1% and a large J-V hysteresis. Steady state and time resolved photoluminescence of thin films showed the good charge extraction dynamics of H1. In addition, H1 shows a large thermal stability and a complete amorphous feature (as evaluated by TGA and DSC), which represents another step important towards improving the long-term stability of perovskite solar cells.*

Thanks to the excellent properties such as high extinction coefficients, large exciton diffusion lengths, and direct bandgap, organic-inorganic lead halide perovskites[1] have become the optimal choice among light absorbers in order to build high efficiency solar cells. Miyasaka et al. reported the use of methylammonium lead iodide as sensitizer in liquid based dye sensitized solar cell, but the high solubility of this material in polar and protonated solvents limited the efficiency and, more importantly, the stability of the devices.[2] Perovskite solar cells (PSC) have now pushed the sunlight power conversion efficiencies (PCEs) beyond 20%.[3] In a typical lead-organo-halide solid state device, in which the perovskite is the light absorber, a hole transport material (HTM) drives the photogenerated holes to the top electrode (usually gold or silver).[4] The importance of the HTM is not limited to the charge transport dynamics but, more interestingly, it has been reported that the properties of the hole conductor play a significant role in the stability of the perovskite layer and thus affecting the long-term performance.[5] The commercially available **Spiro-OMeTAD**[6] still represents the reference material among high performance HTMs, but there is a large range of literature concerning new alternative organic hole conductors.[7] The most notorious **Spiro-OMeTAD**'s Achilles' heel is the laborious and expensive synthetic route that requires at least three steps with low overall yields.[8] Because of this, recent research in the field of new HTMs has moved toward simple and low cost synthetic routes, generally preferring the minimum number of steps, in the range of one or two.[5,9] In general, the key synthetic step involved in the preparation of HTMs consists in a coupling reaction between the donor moiety and the π-bridge, but in evaluating the overall synthetic strategy the procedures for the preparation of the precursors involved into the coupling reaction have to be taken into account. Here we report a novel HTM (**H1**) based on the 1,3,4-oxadiazole ring as the π-bridge unit that was used in conjunction with the deep valence band methylammonium lead bromide perovskite ($MAPbBr_3$), yielding a higher efficiency, and J-V hysteresis-free, than the reference material (**Spiro-OMeTAD**). More importantly, the extremely simple and scalable synthetic route makes this molecule an interesting tool toward solar cell cost reduction. The 1,3,4-oxadiazole moiety is well known in the literature for exhibiting high photoluminescence and electron-accepting properties as well as for its high thermal and hydrolytic stability and resistance to oxidative degradation.[10] 1,3,4-Oxadiazole has also been used as π-spacer in efficient donor-acceptor sensitizers for dye-sensitized solar cells.[11] It has been demonstrated that symmetrically-functionalized oxadiazole derivatives can exhibit both electron and hole transport behaviors, but the introduction of strong electron-donating groups is more likely to give hole conduction properties to the oxadiazole ring.[12]

The optimized synthesis of **H1** involves only one preparative step, the Buchwald-Hartwig cross coupling reaction between commercially available 4-bromo-methoxybenzene and 2,5-bis-(4-aminophenyl)-1,3,4-oxadiazole, and leads to pure **H1** by a simple precipitation of the crude product without the necessity of performing any purification through silica gel chromatography (Scheme 1). The same synthetic approach was also applied to the synthesis of an amine-substituted analogue, compound **H1N,** which was obtained in a yield comparable to that scored for **H1**.

[a] Dr. S. Carli,* Prof. S. Caramori and Prof. C. A. Bignozzi
Department of Chemistry and Pharmaceutical Sciences,
University of Ferrara
44121 Ferrara (Italy)
E-mail: crlsfn@unife.it
[b] Dr. J. P. Correa Baena,* Prof. A. Hagfeldt
Laboratory of Photomolecular Science
Institute of Chemical Sciences and Engineering
Ecole Polytechnique Federale de Lausanne
1015 Lausanne (Switzeralnd)
E-mail: JUAN.CORREA@epfl.ch
[c] Dr. G. Marianetti
Scuola Normale Superiore
56126 Pisa (Italy)
[d] Dr. A. Abate, Prof. M. Grätzel
Laboratory for Photonics and Interfaces
Institute of Chemical Sciences and Engineering
Ecole Polytechnique Federale de Lausanne
1015 Lausanne (Switzeralnd)
[e] Prof. F. Bellina
Department of Chemistry and Industrial Chemistry
University of Pisa
56126 Pisa (Italy)

Supporting information for this article is available on the WWW

This result is an important aspect for future material optimization and processing scaling up.

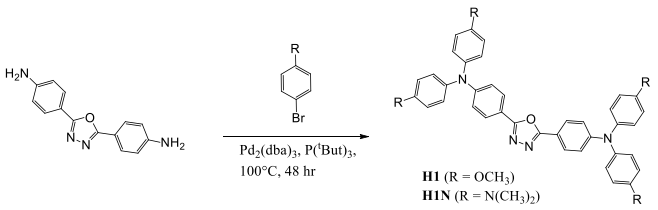

Scheme 1. Synthetic route to the HTMs: **H1** (R = OCH_3), **H1N** (R = $N(CH_3)_2$).

In Figure 1a we report the cyclic voltammetry plot of **H1** and **H1N** in dichloromethane. As it can be observed, **H1** shows a quasi-reversible oxidation peak (see Figure S1 for the full range CV of **H1**), while **H1N** shows the typical two oxidation peaks, corresponding to the one electron oxidation process for each triphenylamine unit.[13] The deeper **H1** HOMO level (-5.46 eV) is presumably ascribed to the 1,3,4-oxadiazole, that consists of an electron-deficient aromatic heterocycle with two nitrogens and one oxygen. A similar structure, for instance, in which the 1,3,4-oxadiazole is replaced by a furane (one oxygen) lead to a higher HOMO energy level, in the order of -5.18 eV.[9c] The UV-Visible and fluorescence emission spectra of **H1** and **H1N** are reported in Figure 1b. Both the oxadiazole derivatives showed similar spectra with absorption peaks located in the spectral window between 380 and 390 nm, with no maximum peaks in the visible region.

From the intersection of emission and absorption spectra we extrapolated the $E_{0\text{-}0}$ transition and, finally, the HOMO-LUMO energy gap. In Table 1 we reported frontier orbital energy levels measured by cyclic voltammetry and UV-Visible absorption/emission.

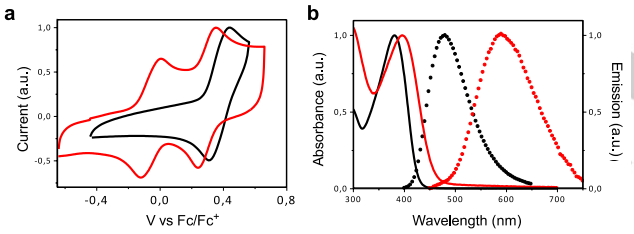

Figure 1. a) Cyclic voltammogram of H1 (black) and H1N (red) in dichloromethane, b) Normalized UV-Visible absorption (line) and emission (dot) of H1 and H1N in chlorobenzene solution.

Table 1. Summary of photophysical and electrochemical properties of **H1** and **H1N** HTMs.

HTM	$E_{1/2}$ (V Vs Fc)	HOMO [a] (eV)	LUMO [b] (eV)	E_{gap} (eV)	λ_{max}, (nm)
H1	+0.36	-5.46	-2.62	2.92	380
H1N	-0.06	-5.06	-2.41	2.56	395

[a] E_{HOMO} (eV)= -[$E_{1/2}$ HTM (Vs Fc/Fc^+) +0.67 + 4.44]
[b] $E_{LUMO} = E_{HOMO} + E_{gap}$

The HOMO and LUMO energy level for **Spiro-OMeTAD** have been reported in the order of -5.22 eV and -2.28 eV respectively, with an energy gap Eg of 2.94 eV.[4,8a] DFT calculations were performed with Gaussian 09, at the B3LYP 6-31 G(d) level of theory in order to clarify the electrochemical and optical properties of **H1** and **H1N**. Calculations at the same level of theory were collected for the **Spiro-OMeTAD** as a reference. DFT calculated HOMO and LUMO energy levels of **H1** and **Spiro-OMeTAD** HTMs, and relative isodensity molecular orbital distribution are reported in Figure 2. **H1N** computed molecular orbital distributions are very similar to **H1** and are reported in Figure S2. While the HOMO is extended between the triphenylamine units and the π-orbitals of the 1,3,4-oxadiazole ring, the LUMO is mainly localized on the 1,3,4-oxadiazole bridge with a strong π-anti-bonding character. It can be argued that the nature of the electron-donating group, methoxy (MeO-) or dimethylamino (NMe_2-) in **H1** and **H1N**, respectively, lead to a slightly major contribution on the resulting energy of the HOMO orbitals, while the LUMO level are less sensitive to electron-donating properties of substituents. Obviously, DFT calculated absolute energy values are slightly different from experimental but the trend is perfectly matched, as can be evaluated in Table 1. The lower energy gap $E_{0\text{-}0}$ observed for **H1N** is presumably ascribed to the higher HOMO destabilization due to the stronger electron donating dimethylamino group.

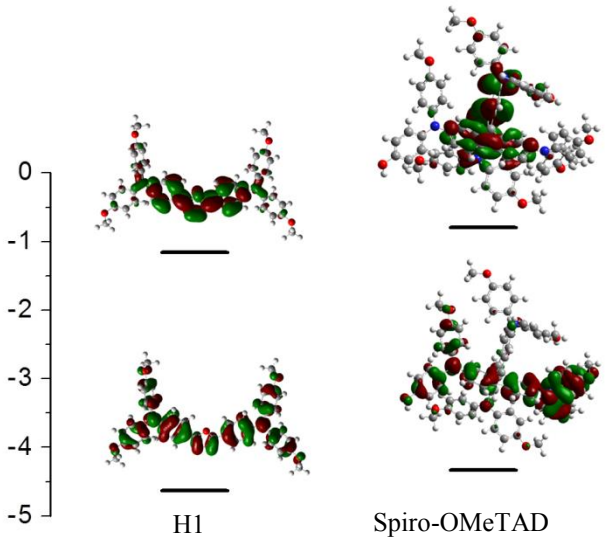

Figure 2. HOMO-LUMO molecular distribution of HTMs at B3LYP/6-31G(d) level of theory performed on vacuum (isodensity = 0.04).

Low lying HOMO level HTMs represent an attractive family of hole conductors that is suitable to obtain high photovoltages from the higher band gap $MAPbBr_3$ (Eg ≈ 2.3 eV[14]). The most promising HTMs used for this purpose are Perylenediimide[15] and carbazolyl[16] derivatives. Thanks to its deeper HOMO level, **H1** (-5.4 eV) is perfectly suitable for matching the low lying VB of $MAPbBr_3$ perovskite (-5.9 eV[14]) Still, LUMO energy levels of **H1** is higher than $MAPbBr_3$ conduction band (in the order of -3.6 eV).[14] This is important in order to avoid competitive electron injection. In Figure 3 we illustrate the J-V curves of a typical $MAPbBr_3$ solar cell using **H1** and the **Spiro-OMeTAD** as HTMs doped with lithium salt Li-TFSI[17] and the cobalt complex

FK209[18], while in Table 2 we report the relative performance parameters. It can be observed that both **H1** and the control **Spiro-OMeTAD** HTMs lead to similar short-circuit current (J_{sc}) and open circuit voltage (V_{oc}) in the order of 5.5-5.8 mA cm^{-2} and 1.43-1.49 V, respectively.

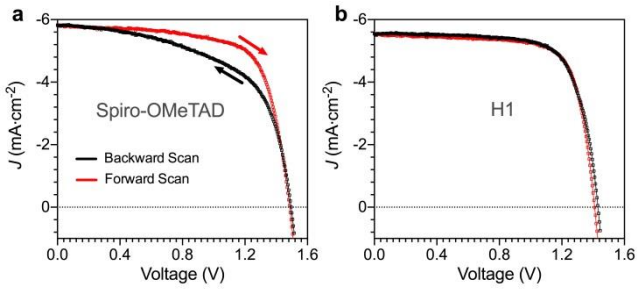

Figure 3. Current-voltage curves of the solar cells prepared with **Spiro-OMeTAD** and **H1** HTMs under AM1.5 simulated sun light. Devices were masked with an aperture of 0.16 cm^2 to define the active area. The curves were recorded with a scan rate of 0.01 V s^{-1} from forward bias to short circuit condition and vice versa.

Table 2. Characteristics data of I−V for **Spiro-OMeTAD** and **H1** solar cells.[a]

HTM	Scan Direction	J_{SC} mA·cm^{-2}	V_{OC} V	FF	PCE %
Spiro-OMeTAD	Backward	5.80	1.49	0.58	5.07
	Forward	5.80	1.49	0.70	6.12
H1	Backward	5.50	1.43	0.72	5.80
	Forward	5.50	1.41	0.73	5.80

[a] *Light intensity: 99.3 mW cm^{-2}*

A typical stack architecture composed of FTO/compact TiO_2/mesoporous TiO_2/$MAPbBr_3$/HTM/gold was used in our study. As seen in the SEM image (see Figure 4), a 200 nm mesoporous TiO_2 is used as the electron selective layer, with a large crystal 700 nm layer of $MAPbBr_3$. The **H1** HTM layer shows a thickness of the HTM layer in the order of 130 nm while the control material **Spiro-OMeTAD** is typically optimized at around 200 nm.

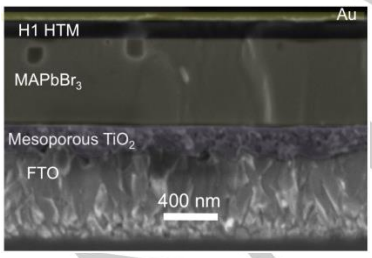

Figure 4. Cross-section scanning electron micrograph of the best device containing the hole conductor **H1**.

H1N exhibited very poor solubility in solvent compatible with the perovskite and it was impossible to get homogeneous layer deposition, such as the case of **H1**. Thus, solar cell devices based on this HTM was not further investigated in this work.

The visible spectrum of the chemically oxidized **H1**, upon addition of the Li-TFSI and FK209 dopants, shows a well-defined new band at 777 nm and two shoulders, with lower intensity, at ca 635 nm and 488 nm that do not compete with the $MAPbBr_3$ absorption, as depicted in Figure S3. To gain a deeper understanding of the charge extraction dynamics at the $MAPbBr_3$ perovskite/**H1** interface, steady-state and time resolved photoluminescence were collected. The typical emission peak at 544 nm of the pristine $MAPbBr_3$[19] upon excitation at 450 nm is almost completely quenched after the deposition of a film of **H1** or **Spiro-OMeTAD** (see Figure S4): the intensity of the peak decreased a factor of 95-98% indicating a good hole transfer and thus an optimal energy alignment at the interface perovskite-HTM.

The high efficient charge pair separation has also been demonstrated through time correlated single photon counting measurements (TCSPC) monitoring the emission at 544 nm. The pristine $MAPbBr_3$ exhibited an emission lifetime τ_e of 18 ns, which is dramatically reduced to 1 ns when the perovskite film is coated with **H1** or **Spiro-OMeTAD** HTMs (as reported in Figure S5).

Thermogravimetric analysis (TGA) was performed in order to evaluate the thermal stability and solid state properties of **H1** and **H1N**. We observed that both **H1** and **H1N** (Figures S6-S7) oxadiazole-based derivatives start to decompose at around 390-400°C indicating a relative high thermal stability of this class of materials. Also, the amorphous nature of **H1** and **H1N** have been confirmed by differential scanning calorimetry (DSC) with a Tg of 85°C (Figure 5) and 150°C (Figure S8), respectively.

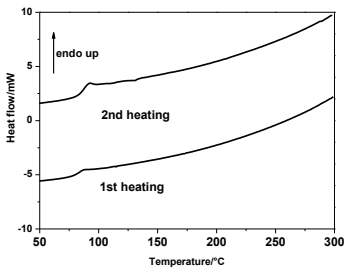

Figure 5. Differential scanning colorimetry (first and second heating curves) of **H1**.

It has been demonstrated that a stable amorphous phase is very important to retain the device performances on a long term, since the crystallization of the HTM reduces the electric contact at the interface with the perovskite and the metal contact.[5,20] For comparison, it has been reported that **spiro-OMeTAD** processed from solution exhibits a glass transition around 150°C and melting of the crystalline phases around 245°C. Moreover, when processed from solution to deposit the HTM layer in solar cells **Spiro-OMeTAD** forms a film predominantly amorphous.[5] However, long time ageing tests have shown the formation of crystalline domains within the amorphous **spiro-OMeTAD** films which are responsible for device performance degradation. From this point of view, **H1** does not exhibit any melting of the crystalline phases leading to potentially higher long time stability.

In conclusion, a new 1,3,4-oxadiazole based HTM (**H1**) was prepared with a one-step synthetic route and tested as HTM in a wide band-gap $MAPbBr_3$ perovskite solar cell. **H1** allows hysteresis free J-V scan with a better efficiency, than the state-of-the-art HMT **Spiro-OMeTAD**. The extremely simple and reproducible synthetic route can be easily extended for the synthesis of other 1,3,4-oxadiazole based HTMs, making this class of compounds very attractive to prepare cost effective HTM with tunable electronic properties.

Acknowledgements

Dr. A. Abate has received funding from the European Union's Seventh Framework Programme for research, technological development and demonstration under grant agreement n° 291771. Dr. Alessio Spepi of the Thermolab Group at the Department of Chemistry and Industrial Chemistry of the University of Pisa (Italy) is gratefully acknowledged for recording DSC and TGA data. Prof. F. Bellina wish to thank the University of Pisa for financial support (PRA 2015, project No. 2015_0038).

Keywords: hole transport materials • perovksites • solar cells • mesoporous materials • solid-state structures

[1] D. B. Mitzi, C. A. Field, W. T. A. Harrison, A. M. Guloy, *Nature* **1994**, *369*, 467-469.

[2] A. Kojima, K. Teshima, Y. Shirai, T. Miyasaka, *J. Am. Chem. Soc.* **2009**, *131*, 6050-6051.

[3] M. A. Green, K. Emery, Y. Hishikawa, W. Warta, E. D. Dunlop, *Prog. Photovolt: Res. Appl.* **2015**, *23*, 1-9.

[4] H. S. Kim, C. R. Lee, J. H. Im, K. B. Lee, T. Moehl, A. Marchioro, S. J. Moon, R. Humphry-Baker, J. H. Yum, J. E. Moser, M. Grätzel, N. G. Park, *Sci. Rep.* **2012**, *2*, 1-7.

[5] A. Abate, S. Paek, F. Giordano, J. P. Correa-Baena, M. Saliba, P. Gao, T. Matsui, J. Ko, S. M. Zakeeruddin, K. H. Dahmen, A. Hagfeldt, M. Grätzel, M. K. Nazeeruddin, *Energy Environ. Sci.* **2015**, *8*, 2946-2953.

[6] U. Bach, D. Lupo, P. Comte, J. E. Moser, F. Weissortel, J. Salbeck, H. Spreitzer, M.Grätzel, *Nature* **1998**, *395*, 583-585.

[7] Z. Yu, L. Sun, *Adv. Energy Mater.* **2015**, doi:10.1002/aenm.201500213.

[8] (a) N. J. Jeon, H. G. Lee, Y. C. Kim, J. Seo, J. H. Noh, J. Lee, S. I. Seok, *J. Am. Chem. Soc.* **2014**, *136*, 7837-7840. (b) K. Zhang, L. Wang, Y. Liang, S. Yang, J. Liang, F. Cheng, J. Chen, *Synth. Met.* **2012**, *162*, 490-496.

[9] (a) H. Li, K. Fu, A. Hagfeldt, M. Grätzel, S. G. Mhaisalkar, A. C. Grimsdale, *Angew. Chem. Int. Ed.* **2014**, *53*, 1-5. (b) P. Gratia, A. Magomedov, T. Malinauskas, M. Daskeviciene, A. Abate, S. Ahmad, M. Grätzel, V. Getautis, M. K. Nazeeruddin, *Angew. Chem. Int. Ed.* **2015**, *54*, 1-5. (c) A. Krishna, D. Sabba, J. Yin, A. Bruno, P. P. Boix, Y. Gao, H. A. Dewi, G. G. Gurzadyan, C. Soci, S. G. Mhaisalkar, A. C. Grimsdale, *Chem. Eur. J.* **2015**, *21*, 1-6.

[10] (a) J. Bettenhausen, M. Greczmiel, M. Jandke, P. Strohriegl, *Synth. Met.* **1997**, *91*, 223-228. (b) J. A. Mikroyannidis, I. K. Spiliopoulos, T. S. Kasimis, A. P. Kulkarni, S. A. Jenekhe, *Macromolecules* **2003**, *36*, 9295-9302. (c) C. Wang, G. Y. Jung, Y. Hua, C. Pearson, M. R. Bryce, M. C. Petty, A. S. Batsanov, A. E. Goeta, J. A. K. Howard, *Chem. Mater.* **2001**, *13*, 1167-1173.

[11] K. Srinivas, G.Sivakumar, Ch.Ramesh Kumar, M. Ananth Reddy, K. Bhanuprakash, Rao, V. Jayathirtha, C. W. Chen, Y. C. Hsu, J. T. Lin, *Synth. Met.* **2011**, *161*, 1671-1681.

[12] H. Tokuhisa, M. Era, T. Tsuitsui, S. Saito, *Appl. Phys. Lett.* **1995**, *66*, 3433-3435.

[13] M. Planells, A. Abate, D. J. Hollman, S. D. Stranks, V. Bharti, J. Gaur, D. Mohanty, S. Chand, H. J. Snaith, N. Robertson, *J. Mat. Chem. A* **2013**, *1*, 6949-6960.

[14] P. Schulz, E. Edri, S. Kirmayer, G. Hodes, D. Cahen, A. Kahn, *Energy Environ. Sci.* **2014**, *7*, 1377-1381.

[15] J. Das, R. B. Siram, D. Cahen, B. Rybtchinski, G. Hodes, *J. Mater. Chem. A* **2015**, *3*, 20305-20312.

[16] E. Edri, S. Kirmayer, M. Kulbak, G. Hodes, D. Cahen, *J. Phys. Chem. Lett.* **2014**, *5*, 429-433.

[17] A. Abate, T. Leijtens, S. Pathak, J. Teuscher, R. Avolio, M. E. Errico, J. Kirkpatrik, J. M. Ball, P. Docampo, I. McPhersonc, H. J. Snaith, Phys.Chem. Chem. Phys., **2013**, *15*, 2572-2579.

[18] J. Burschka, F. Kessler, M. K. Nazeeruddin, M. Grätzel, *Chem. Mater.* **2013**, *25*, 2986-2990.

[19] (a) M. Zhang, H. Yu, M. Lyu, Q. Wang, J. H. Yun, L. Wang, *Chem. Commun.* **2014**, *50*, 11727-11730. (b) F. C. Hanusch, E. Wiesenmayer, E. Mankel, A. Binek, P. Angloher, C. Fraunhofer, N. Giesbrecht, J. M. Feckl, W. Jaegermann, D. Johrendt, T. Bein, P. Docampo, *J. Phys. Chem. Lett.* **2014**, *5*, 2791-2795.

[20] T. Malinauskas, D. Tomkute-Luksiene, R. Sens, M. Daskeviciene, R. Send, H. Wonneberger, V. Jankauskas, I. Bruder, V. Getautis, *Appl. Mater. Interfaces* **2015**, *7*, 11107-11116.

Entry for the Table of Contents
Layout 1:

COMMUNICATION

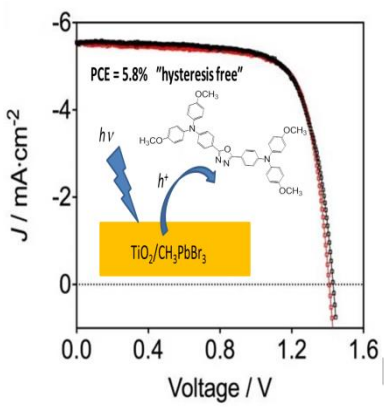

Stefano Carli, Juan Pablo Correa Baena,* Giulia Marianetti, Antonio Abate Stefano Caramori, Michael Grätzel,Fabio Bellina, Carlo Alberto Bignozzi, Anders Hagfeldt*

Page No. – Page No.

A New 1,3,4-Oxadiazole-based Hole Transport Material for Efficient $CH_3NH_3PbBr_3$ Perovskite Solar Cells: Facile Synthesis and Energy Level Alignment.

1,3,4-oxadiazole moiety has been used as π-spacer to prepare a new HTM (H1). This compound was tested in on $CH_3NH_3PbBr_3$ perovskite solar cells yielding "hysteresis free" JV and PCE% higher than the reference material (Spiro-OMeTAD). Thanks to the extremely simple synthetic route this is an important goal in order to obtain high performance perovskite solar cells, while reducing costs.